Research Square

Preprints are preliminary reports that have not undergone peer review.
They should not be considered conclusive, used to inform clinical practice,
or referenced by the media as validated information.

Foot Segments Motion during Uneven Terrain Walking and Influence on Lower Limb Biomechanics

Anna Pace

anna.pace@iit.it

Italian Institute of Technology

Matteo Crotti

Italian Institute of Technology

Gabriele Gervasi

Sapienza University of Rome

Giorgio Grioli

Italian Institute of Technology

Eduardo Palermo

Sapienza University of Rome

Antonio Bicchi

Italian Institute of Technology

Manuel Giuseppe Catalano

Italian Institute of Technology

Article

Keywords:

Posted Date: March 9th, 2026

DOI: https://doi.org/10.21203/rs.3.rs-8712582/v1

License: This work is licensed under a Creative Commons Attribution 4.0 International License.
Read Full License

Additional Declarations: No competing interests reported.

Version of Record: A version of this preprint was published at Scientific Reports on September 5th, 2026.
See the published version at https://doi.org/10.1038/s41598-026-61350-8.

Foot Segments Motion during Uneven Terrain Walking and Influence on Lower Limb Biomechanics

Anna Pace[1,+,*], Matteo Crotti[1,2,+], Gabriele Gervasi[3], Giorgio Grioli[1,2], Eduardo Palermo[3], Antonio Bicchi[1,2], and Manuel G. Catalano[1]

[1]Soft Robotics for Human Cooperation and Rehabilitation, Istituto Italiano di Tecnologia, Genoa 16163, Italy.
[2]Department of Information Engineering and Research Center "E. Piaggio," University of Pisa, Pisa 56122, Italy.
[3]Department of Mechanical and Aerospace Engineering, Sapienza University of Rome, Rome 00184, Italy.
[*]corresponding author: anna.pace@iit.it
[+]these authors contributed equally to this work

ABSTRACT

Human locomotion has been extensively studied on flat ground; however, everyday walking often occurs on uneven terrain, which poses additional biomechanical challenges. The role of foot segmental mobility under these conditions remains underexplored. This study investigated how irregular surfaces influence foot kinematics and lower-limb biomechanics. Twelve able-bodied young adults performed eight barefoot tasks at self-selected speed, including level walking, obstacle crossing, walking on uneven ground, ramp, and stairs. Kinematic data were collected using the multi-segment Oxford Foot Model, and hip, knee, and ankle biomechanics were analyzed to identify compensatory strategies. Participants exhibited increased plantarflexion of the hallux and forefoot, increased dorsiflexion of the forefoot and hindfoot relative to the tibia, and a reduced range of motion of the foot segments, suggesting a stiffening strategy to enhance grip and stability. Ankle range of motion decreased, while knee and hip flexion slightly increased throughout stance. Kinetically, ankle plantarflexor torque increased during the first half of stance, whereas push-off torque and power were reduced. Concurrently, negative power absorption at the knee increased, confirming its role as a mechanical damper. Overall, these findings highlight a redistribution of joint function and the pivotal role of foot segments and ankle dynamics in enabling stable locomotion on uneven terrain.

Introduction

Humans move through diverse and often complex environments in their everyday lives. Whether on an uneven sidewalk or a rugged natural trail, people frequently encounter surfaces challenging smooth movement. Terrain affects locomotion in many ways, and the foot is the first body part interacting with it, accommodating ground features to provide stable navigation.

This adaptive capability is the result of a long evolutionary process for enhanced long-distance walking and running[1]. Contrary to common wisdom, the midfoot joints exhibit, on average, greater motion than our ancestors, the chimpanzees, during the stance phase of walking (i.e. when the foot is in contact with the ground)[2]. In particular, the human foot shows larger plantarflexion (i.e. sagittal-plane rotation of the foot or a distal foot segment away from the tibia or the adjacent proximal segment, toward the plantar surface) and adduction (i.e. medial rotation of the distal segment in the transverse plane) of the midfoot joints during push-off (i.e. when the foot prepares to leave the ground and the heel is lifted). The foot's complex anatomy ensures impact absorption and stiffness modulation for balance and locomotion across all terrains and tasks. Multiple foot joints filter larger ground irregularities, allowing the foot to conform to the ground profile, while the soft tissue padding covering the bony structure filters smaller ones[3].

Although the critical role of foot articulations in ensuring stable gait on flat and uneven terrains is widely acknowledged, the literature still lacks comprehensive biomechanical studies investigating foot deformation over obstacles or uneven terrains and its relationship with the ankle, knee, and hip joints. Several studies have examined adaptations at proximal joints, but typically model the foot as a single rigid segment, potentially skewing our understanding of biological foot function[4]. Conversely, multi-segment foot models are increasingly adopted in clinical practice, yet have rarely been applied or validated in the context of uneven terrain walking.

Research work on gait on uneven-surface treadmills reported increased step variability with largely preserved gait kinematics, greater knee and hip mechanical work, and a 28% rise in net metabolic rate[5]. Similarly, running on uneven surfaces increased energy expenditure with modest changes in joint kinetics and kinematics, with the most notable adaptations at the ankle[6]. Outdoor studies (e.g. gravel, grass, woodchips) further highlighted terrain-dependent adjustments, including stride parameter variability, altered energy expenditure, and changes in foot clearance[7]. On loose rock, individuals increased hip and knee flexion early in stance - along with landing with a flatter foot - and during swing - while also increasing ankle dorsiflexion, to lower the

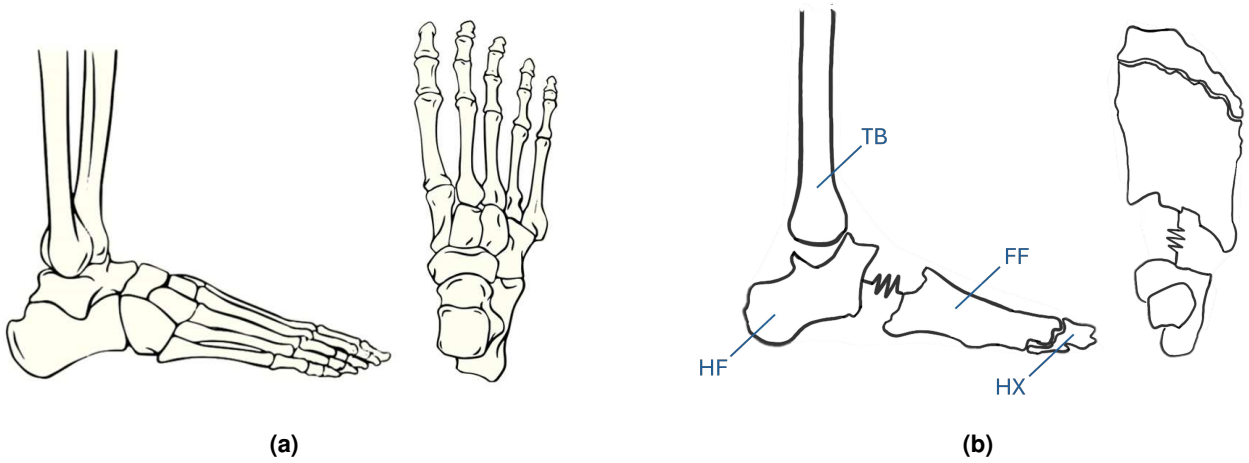


Figure 1. The human foot and its modeling for gait analysis. Sagittal and transverse views of (a) the human foot skeleton and (b) the corresponding three rigid foot segments of the Oxford Foot model: hindfoot (HF), forefoot (FF), and hallux (HX). The tibia (TB) is also shown.

centre of mass for stability and increase toe clearance respectively, despite maintaining consistent step parameters[8]. All these studies used motion-capture-based gait analysis - still the gold standard for investigating human gait - on indoor-replicated uneven grounds (with one exception using inertial measurement units outdoors[7]), but treated the foot as a single segment, focusing on adaptations at the ankle, knee, and hip.

Various multi-segment models have been developed, dividing the foot into a variable number of segments according to the desired anatomical faithfulness[9–13]. They are widely used in clinical applications to study foot functionality and identify the foot kinetics and kinematics in healthy and pathological individuals[10–12,14–18], as well as for performance analysis[19,20]. The choice of foot model affects not only foot information but also proximal joint kinematics[21]. The Oxford Foot Model is a widely used three-dimensional multi-segment foot model including hindfoot, forefoot, and hallux[22–24] (Fig. 1). Despite not explicitly modelling the midfoot (considered as a force transmitter between hindfoot and forefoot), its repeatability has been validated in children and adults. It was used in several clinical studies[25–30], as well as to investigate foot kinematics in various dynamic tasks[20,31,32]. Moreover, its cross-centre reliability and the availability of post-processing software facilitate large-cohort studies[23].

The present study aimed to quantify foot kinematics and kinetics in healthy adults walking on uneven grounds. We performed motion-capture gait analysis while participants walked indoors on terrains simulating real-world scenarios (e.g. trails with stones, twigs, branches, cobblestone paths, etc.). The Oxford Foot Model was used to analyze foot mobility, combined with a lower-body model to track the complete lower-limb biomechanics. We hypothesized the following compensatory strategies adopted by the limb stepping on the obstacle, particularly in the first half of stance, which is when the foot approaches and accommodates for the ground profile: (i) increased motion of foot segments, specifically greater dorsiflexion of proximal foot segments relative to the tibia and greater plantarflexion of distal segments relative to proximal ones; (ii) reduced ankle range of motion (ROM) as hindered by the obstacles; (iii) increased ankle moment; (iv) increased knee flexion to step on obstacles and higher negative knee power peaks to dissipate more energy during flexion.

Understanding foot biomechanics on uneven terrains is essential for interpreting human locomotion in real-world conditions, contributing to the broader field of human motor control. This knowledge is also crucial to inform the design and control of adaptive artificial feet for prostheses and bipedal robotic systems, which draw inspiration from human foot anatomy and gait strategies to achieve adaptability and stability across diverse environments.

Methods

Participants

Twelve healthy individuals (8 male, 4 female, 77.8 ± 15.8 kg, 1.78 ± 0.07 m, 27.8 ± 6.3 y/o) participated in the study. Inclusion criteria comprised being adult individuals without impairment, conducting an active lifestyle, and ability to participate in the experimental activity (the experiment lasted approximately 2 hours). Exclusion criteria included any pathologies or disabilities affecting the walking ability and interfering with the experimental procedure. All the participants matched the inclusion criteria, and they gave their informed written consent to the experimental activity, which was conducted according to the Declaration of Helsinki, and approved by the Bioethical Committee of the University of Pisa (resolution no. 48/2024).

Experimental setup

A 12-camera motion capture system (Vicon Motion Systems Ltd., Oxford, UK) was used to collect kinematic data at 100 Hz. A set of 26 passive reflective markers was placed on bony landmarks of the participants' feet according to the Oxford Foot Model[22] (Fig. 2): lateral fibula heads, tibial tuberosities, anterior aspects of the shin, medial malleoli, posterior ends of the calcanei, posterior calcanei proximal, lateral calcanei, sustaniculum tali, the first and fifth metatarsals - both proximal and distal, lastly on the halluces. Additional 16 markers were placed on the lower limbs according to the lower-limb Plug-in Gait model, which is embedded in the Vicon system, and it is based on the Newington-Helen Hayes gait model[24,33]. Specifically, markers were placed on the anterior and posterior superior iliac spines, the lateral surface of the thighs, the lateral knee axes, the the lateral surface of the shanks, the lateral malleoli, the calcanei, and the second metatarsal heads. Two force plates (60x120 cm, AMTI, Watertown, MA, USA) embedded in the ground were used to measure ground reaction forces (GRFs) at 1 kHz.



Figure 2. Marker set used for the experimental activity. On the left, markers placed on the lower limbs according to the lower-limb Plug-in Gait model, and on the foot according to the Oxford Foot model; on the right, magnified view of the feet. EMG data from sensors placed on the lower limbs are not used in this study.

In addition, three wooden obstacles with different shapes (arch, rectangle, and circle) and uneven wooden panels were used (Fig. 3)[34]. In particular, $h_{arch} > h_{rect} > h_{circle} > max(h_{uneven})$, where $max(h_{uneven})$ represents the maximum height difference between the bottom and top wooden layer of the uneven panels.

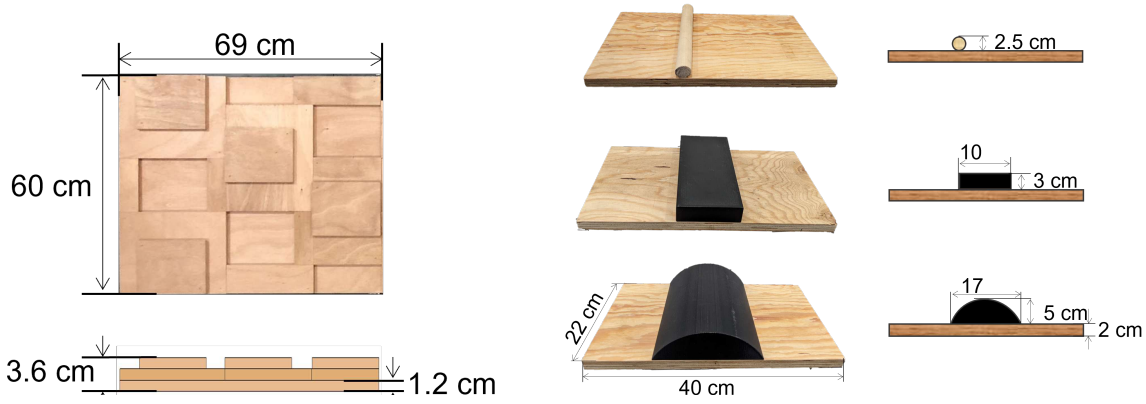


Figure 3. On the left, uneven wooden panel ($1.2\,cm < h_{uneven} < 3.6\,cm$); on the right, wooden obstacles: from top to bottom, circular ($h_{circle} = 2.5\,cm$), rectangular ($h_{rect} = 3\,cm$), and arched ($h_{arch} = 5\,cm$).

Experimental protocol

Participants were asked to perform eight tasks barefoot and at self-selected walking speed: walking on level ground; walking while stepping on the three differently-shaped obstacles; walking on uneven ground; walking on stairs; walking on a ramp. Obstacles were placed on one of the force plates. The uneven-ground task was implemented in two configurations: first, two wooden panels were used, with one panel placed on each force plate (hereafter referred to as *uneven*); second, four wooden panels were assembled in a row to form a walkway, bypassing the force plates (hereafter referred to as *uneven4line*). Ten valid trials (i.e. clean foot strike on the force plates) were collected for each task. As for the obstacles, participants were asked to step on each obstacle, five trials with one foot and the other five with the contralateral foot.

While prior studies often standardized walking velocity to ensure comparability, the present study prioritized the preservation of natural gait dynamics. A predetermined velocity was not imposed, as constraining participants to an artificial pace has been shown to markedly alter gait characteristics and compromise stability[35]. Conversely, self-selected walking speed better reflects real-world overground conditions, where no predetermined speed is enforced[36].

Data analysis

Raw kinematic and kinetic data were filtered in Vicon Nexus v.2.12.1 by using a zero-lag, fourth-order, low-pass Butterworth filter, with a cut-off frequency of respectively 10Hz for markers' trajectories and 20Hz for GRF data. Inverse kinematics and dynamics were also conducted in Vicon Nexus.

Matlab (v.R2024b, MathWorks Inc., Natick, MA, USA) was used to display results. Joint torques are normalised to the body mass and displayed as internal ones (due to muscle and joint contact forces) opposing the external torques generated by the GRF[37]. The GRF components are displayed as a percentage of the subjects' body weight (%BW). Kinematic and kinetic variables are normalized to the stride duration, and resampled to 200 samples.

Statistical analysis

A descriptive statistical analysis was conducted in Matlab, calculating mean values ($\pm$ 1SD) of angles, torques, and powers across the 10 valid trials within each subject first and then inter-subject.

Afterwards, an inferential statistical analysis was conducted to compare angle and torque profiles throughout the gait cycle during walking on level and non-flat grounds by means of the statistical parametric mapping technique, using the Statistical Parametric Mapping *spm1d* package (v M.0.4.10, www.spm1D.org) in Matlab. The normality assumption on the residual was tested with the Shapiro-Wilk test and was not satisfied. Hence, a non-parametric paired two-tailed t-test ($\alpha = 0.05$) was performed. A statistically significant difference between the two angle or torque patterns was found whenever the $SPM\{t\}$ statistics crossed the null hypothesis rejection threshold (resulting p-values in Table 1).

Moreover, a repeated measures analysis of variance (ANOVA) was conducted to evaluate differences in kinematic and kinetic parameters across the tested experimental conditions. Given a significant main effect of condition, planned pairwise comparisons were conducted between the baseline condition (level ground walking) and each of the remaining conditions. Post hoc pairwise comparisons were conducted using Tukey's honestly significant difference (HSD) method to identify specific differences between conditions while controlling for the family-wise error rate. Statistical significance was defined as $p < 0.05$.

To assess potential confounding effects of walking speed in kinematic and kinetic variables between conditions, mean walking speed was computed for each subject and condition and normalized to leg length using the Froude number ($Fr = v^2/(gL)$) (see Supplementary Tables S1 and S2 for walking speed and Froude values for each subject and condition). For each non-flat condition, subject-specific changes in Froude values relative to level walking were calculated. Moreover, Froude values were compared across conditions using a one-way repeated-measures ANOVA, to determine whether subjects walked at comparable normalized speeds across conditions. Lastly, subject-specific changes in Froude number between each non-flat condition and level walking were correlated with changes in some selected sagittal kinematic (range of motion of the hip, knee, and ankle joints, minimum and maximum values of the hip, knee, and ankle angles, as well as of the foot joints angles) and kinetic (the two peaks of the vertical component of the GRF) parameters. Specifically, Spearman's rank correlation ($\alpha = 0.05$) was used for this purpose. These analyses were performed to check whether between-condition differences in biomechanical variables could be attributed to variations in normalized walking speed.

Results

Results are reported in two sections: kinematics and dynamics. Kinematics includes inter-segment foot angles (Fig. 4) and lower-limb joints angles (Fig. 5). Dynamics includes GRF components (Fig. 6), and torque and power profiles for the hip, knee, and ankle joints (Fig. 5). Standard deviations are omitted in Figs. 4 and 5 for clarity and readability. Table 2 reports joint ROM, and selected local maxima/minima of joint angles, torques, powers, and of GRFs. Foot inter-segment rotations are reported in all three anatomical planes. Hip, knee, and ankle kinematics and kinetics are reported in the sagittal plane, where the largest variations occur. Frontal and transverse data, as well as stairs and ramp tasks, are provided in Supplementary Figs. S1-S3.

Regarding walking speed, changes in Froude number for each participant with respect to level walking were generally small (Supplementary Table S2): only one subject showed a change greater than 0.05 in two obstacle conditions. Mean Froude number did not differ across conditions ($p > 0.05$), indicating that subjects walked at dynamically comparable speeds. Correlations between changes in Froude number and changes in selected parameters were non-significant for all variables except isolated cases with no consistent patterns across joints or obstacles (Table 2): $p < 0.05$ for minimum ankle and knee angles - circular obstacle, minimum hip angle - uneven terrain, minimum and maximum hallux-to-forefoot angle - rectangular and circular obstacles, and circular obstacle and uneven terrain respectively, and stance minimum hindfoot-to-tibia angle - arched obstacle.

Kinematics

Navigating uneven terrains and stepping on obstacles induced a reduction of the range of motion of lower-limb joints and foot segments.

Hallux-to-Forefoot

In the sagittal plane, stepping on obstacles increased hallux plantarflexion (PF) relative to the forefoot throughout the gait cycle (GC), with significant differences during loading response (typically 3%-12% of GC) for all obstacles ($p < 0.02$) and during the second half of stance for the rectangle ($p < 0.001$). Walking on irregular grounds mainly affected push-off: the dorsiflexion (DF) peak around toe-off was greatly reduced for all grounds ($p \leq 0.016$ at 60% of GC for the two uneven grounds, the rectangular and arched obstacles). In the frontal plane, the profile was similar across conditions, with decreased eversion during single limb support for arch/rectangle obstacles and increased eversion on uneven terrains. In the transverse plane, profiles were comparable, with slightly increased stance adduction for rectangular/circular obstacles and reduced abduction close to toe-off.

On the ramp and stairs, the DF peak around toe-off was reduced compared with level walking, with the smallest peak occurring during downhill walking (Supplementary Fig. S2).

Forefoot-to-Hindfoot

In the sagittal plane, forefoot PF relative to the hindfoot increased for most of stance on uneven grounds and mainly during the second half of stance on obstacles. The PF peak around toe-off was reduced particularly during obstacle negotiation ($p \leq 0.025$ for all three obstacles at about 60% of GC). ROM was significantly reduced for all tested conditions compared with level ground. In the frontal plane, ROM decreased for all conditions; supination and pronation peaks decreased on obstacles around 50% of GC and toe-off ($p \leq 0.016$ at about 60% of GC for rectangle and arch). During the first half of stance, supination increased for arch and rectangle compared with level walking ($p \leq 0.024$ before 10% of GC). In the transverse plane, there was a tendency toward abduction on obstacles, with an opposite trend around toe-off and throughout stance for uneven grounds.

During stair and ramp ascent, forefoot-to-hindfoot DF generally increased, with an opposite trend around toe-off of stair ascent and during the loading response in stair descent. In contrast, stance DF decreased during ramp descent and, together with stair descent, did not exhibit a plantarflexion peak around 60% of GC (Supplementary Fig. S2).

Hindfoot-to-Tibia

Sagittally, hindfoot-to-tibia dorsiflexion increased across non-flat grounds. The higher the obstacle (with the arch being the highest), the more pronounced the lack of initial plantarflexion during loading response and the tendency toward dorsiflexion ($p \leq 0.002$ for the three obstacles). ROM was slightly reduced. In the frontal plane, eversion increased on obstacles during stance before push-off; in the transverse plane, external rotation increased throughout stance on all non-flat surfaces.

During uphill walking and stair negotiation, stance dorsiflexion increased (Supplementary Fig. S2). However, during downhill walking or stair descent, a reduced PF peak was observed around toe-off.

Forefoot-to-Tibia

Stepping on obstacles reduced forefoot-to-tibia ROM compared with level walking. Sagittally, plantarflexion decreased during loading response (absent for the arch, $p < 0.001$), while dorsiflexion increased during mid-stance ($p \leq 0.001$; mid-stance typically 12%-31% of GC[38]). Effects increased with obstacle height. The plantarflexion peak during loading response tended to occur earlier, while subsequent peaks were slightly shifted forward in time and reduced for all non-flat terrains ($p \leq 0.006$ at approximately 60% of GC), with significant differences in plantarflexion. Frontally, pronation increased on non-flat grounds between 20% and 50% of GC ($p \leq 0.006$ for circular and arched obstacles), while it decreased on uneven grounds before 20% of GC and from 40% onwards. Transversally, adduction was reduced for all non-flat grounds during loading response ($p < 0.001$), and it resulted in abduction on obstacles until push-off.

The forefoot-to-tibia angle showed a similar trend to that of the hindfoot-to-tibia when negotiating stairs and the ramp (Supplementary Fig. S2).

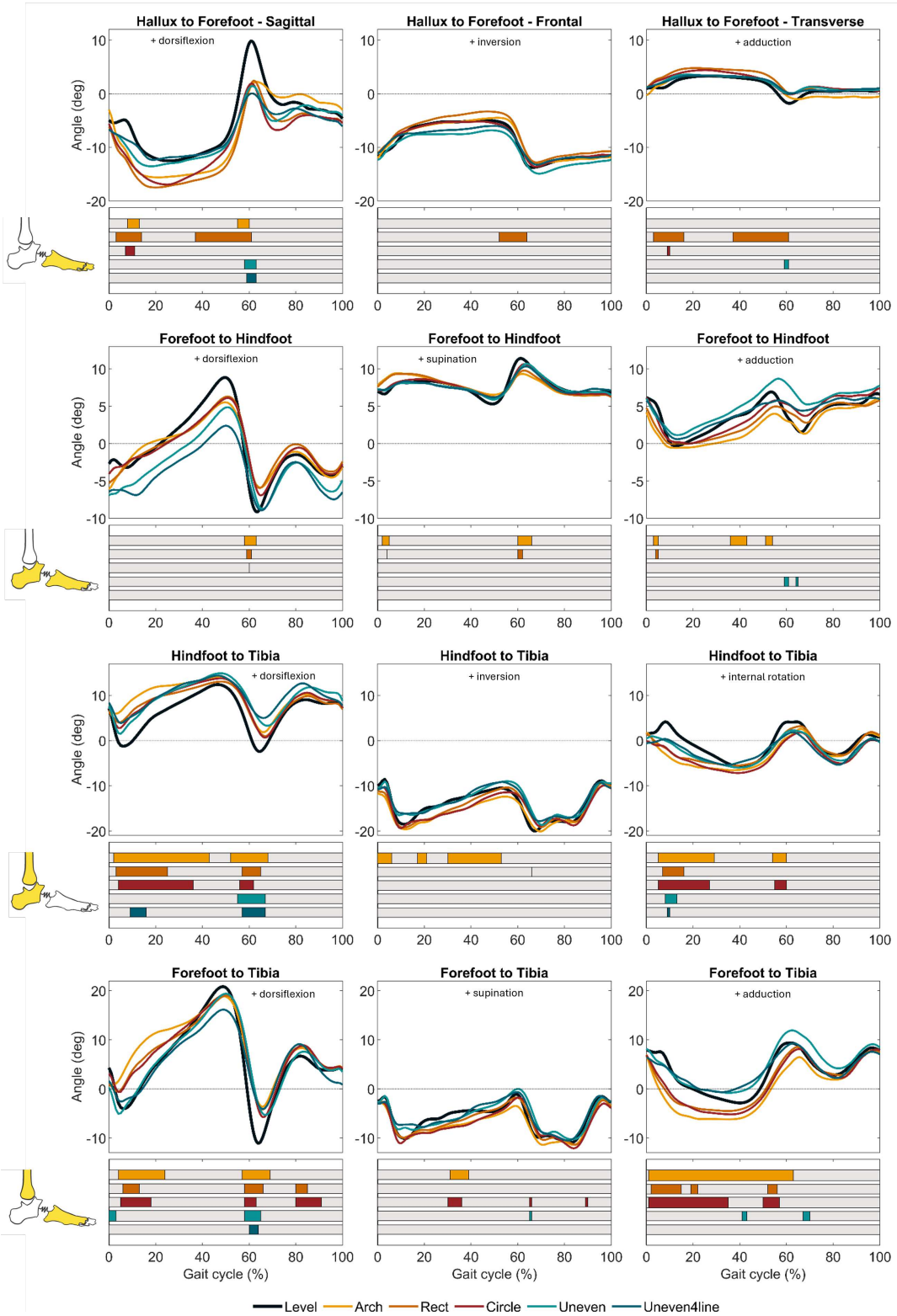


Figure 4. Mean values of angles in the three anatomical planes between the three rigid segments of the foot and the tibia, as defined in the Oxford Foot model. From top to bottom, hallux-to-forefoot, forefoot-to-hindfoot, hindfoot-to-tibia, and forefoot-to-tibia angles. From left to right, rotations in the sagittal, frontal, and transverse planes. The corresponding anatomical segments of the foot are also shown. Data are displayed normalised to stride duration. A non-parametric paired two-tailed t-test ($\alpha = 0.05$) was performed between the angle profiles for each non-flat condition and level walking: coloured bars indicate regions of the gait cycle with statistically significant differences.

Ankle

In the sagittal plane, non-flat conditions led to almost no plantarflexion throughout stance (Fig. 5). Dorsiflexion increased during mid-stance on obstacles ($p \leq 0.001$ for rectangle and arch). The DF peak was similar across all grounds, whereas the PF peak was markedly reduced compared with level walking ($p \leq 0.002$). Frontally and transversally, obstacles were associated with increased stance eversion and external rotation, respectively (Supplementary Fig. S1).

Knee

In the sagittal plane, knee flexion increased during stance on all non-flat grounds until push-off ($p < 0.001$ up to 40% of GC), with larger flexion peaks and reduced extension peaks. The swing flexion peak also increased on non-flat grounds ($p \leq 0.001$ from 70% of GC onwards). Frontal-plane data showed increased abduction on all non-flat grounds until 55% of GC and during swing (Supplementary Fig. S1).

Hip

The sagittal hip angle shifted toward increased flexion in the first half of stance across all conditions ($p < 0.001$) and reduced extension in the second half. Frontally, hip adduction decreased overall on all non-flat grounds except for the arched obstacle (Supplementary Fig. S1).

Dynamics

The condition with four uneven panels in a row is not included here because GRF could not be measured.

Ground Reaction Force

On non-flat grounds, GRF profiles in the three planes retained the typical level-walking pattern (Fig. 6). However, the vertical component of the GRF (vGRF) showed a slightly delayed first peak (notably for the circular obstacle and uneven wooden panels) and a significantly reduced second peak around body weight across all non-flat conditions (Table 2). The medio-lateral GRF (mlGRF) slightly increased overall, whereas peak values of the antero-posterior GRF (apGRF) decreased for the circular obstacle and uneven ground.

Ankle Moment

Non-flat conditions increased ankle plantarflexor moment in the first half of stance ($p \leq 0.001$ between 5% and 25% of GC for uneven terrain and rectangular/arched obstacles) (Fig. 5). The plantarflexor moment decreased compared with level walking in terminal stance (usually $31-50$% of GC[38]), resulting in a reduced moment peak ($p \leq 0.002$ for all non-flat grounds between 40% and 50% of GC). In the frontal plane, an initial eversion moment followed by a reduced inversion moment was observed during stance (Supplementary Fig. S1(a)).

Knee Moment

The extensor peak was slightly greater around 10% of GC on obstacles, but not on uneven ground (Fig. 5). Reduced stance knee extension was mirrored by a reduced flexor moment ($p \leq 0.001$ at about 40% of GC for all non-flat conditions). Uneven terrain showed a temporal shift in the flexor moment peak around 40% of GC. In the frontal plane, the knee moment exhibited a reduced internal abductor moment on all non-flat grounds (Supplementary Fig. S1(a)). On obstacles, indeed, increased ankle eversion tended to induce knee abduction, which was counteracted by an internal adductor moment, resulting in a reduced abductor moment.

Hip Moment

Sagittal hip moment profiles were similar between grounds, with slightly increased extensor moment during mid-stance and slightly reduced flexor moment in terminal stance (Fig. 5). In the frontal plane, the reduced adduction on all non-flat grounds led to a reduced abductor moment (Supplementary Fig. S1(a)).

Power at the Joints

Overall, less power was generated in all non-flat tasks than in level walking, particularly at the ankle during push-off, while knee and hip exhibited larger absorption peaks (Fig. 5).

At the ankle, on obstacles, energy absorption increased during controlled plantarflexion, the negative power then decreased, and push-off power generation was considerably reduced - related to the reduced PF moment (Table 2). At the knee, energy dissipation increased during obstacle negotiation due to the increased flexion moment: the negative power peaks increased during initial stance and push-off. At the hip, obstacles increased energy absorption at the beginning of the gait cycle, whereas uneven terrain was more similar to level walking.

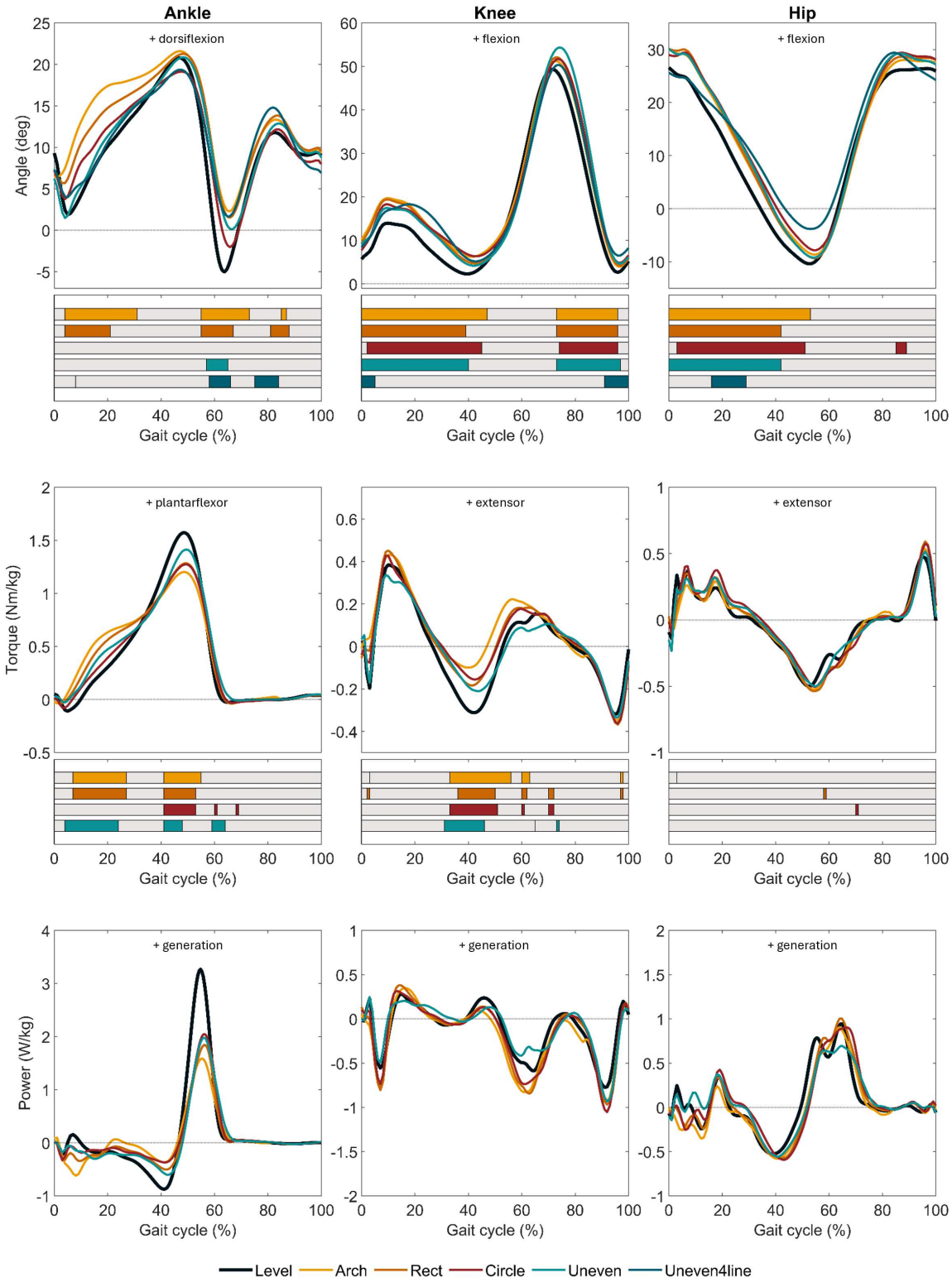


Figure 5. Mean values of angles, torques, and powers (from top to bottom) in the sagittal plane for the ankle, knee, and hip joints (from left to right). Data are displayed normalized to stride duration. Torque and power are normalized to the participant's body mass. A non-parametric paired two-tailed t-test ($\alpha = 0.05$) was performed between the angle and torque profiles for each non-flat condition and level walking: coloured bars show regions of the gait cycle with statistically significant differences.

	p-values					
	Hallux-to-Forefoot Angles			**Forefoot-to-Hindfoot Angles**		
	sagittal	*frontal*	*transverse*	*sagittal*	*frontal*	*transverse*
arch	0.012; 0.008	-	-	0.020	0.008; 0.001	0.013; 0.002; 0.014
rect	0.002; <0.001	0.003	0.003; <0.001	0.013	0.024; 0.016	0.016
circle	0.016	-	0.023	0.025	-	-
uneven	0.004	-	0.015	-	-	0.016; 0.019
uneven4line	0.016	-	-	-	-	-

	Hindfoot-to-Tibia Angles			**Forefoot-to-Tibia Angles**		
	sagittal	*frontal*	*transverse*	*sagittal*	*frontal*	*transverse*
arch	<0.001; 0.001	0.003; 0.006; <0.001	0.001; 0.003	<0.001; 0.001	0.004	<0.001
rect	0.001; 0.007	0.018	0.004	0.001; 0.001; 0.005	-	0.001; 0.018; 0.010
circle	0.002; 0.009	-	<0.001; 0.012	<0.001; 0.004; 0.001	0.006; 0.011; 0.012	<0.001; 0.005
uneven	0.001	-	0.007	0.001; <0.001	0.019	0.019; 0.012
uneven4line	0.014; 0.006	-	0.020	0.006	-	-

	Ankle		**Knee**		**Hip**	
	Angle	Torque	Angle	Torque	Angle	Torque
	sagittal		*sagittal*		*sagittal*	
arch	<0.001; <0.001; 0.017	0.001; <0.001	<0.001; 0.001	0.010; <0.001; 0.002; 0.010	<0.001	0.021
rect	0.001; <0.001; 0.004	0.001; <0.001	<0.001; <0.001	0.002; 0.001; 0.003; 0.002	<0.001	0.008
circle	-	<0.001; 0.009; 0.012	<0.001; 0.001	<0.001; 0.011; 0.004	<0.001; 0.016	0.008
uneven	0.001	<0.001; 0.002; 0.003	<0.001; <0.001	<0.001; 0.014; 0.005	<0.001	-
uneven4line	0.024; 0.002; 0.004	na	0.005; 0.001	na	0.002	na

Table 1. P-values resulting from the non-parametric paired two-tailed t-test ($\alpha = 0.05$) performed between the angle and torque profiles for each non-flat condition and level walking. They are associated with the coloured bars of Figs. 4 and 5.

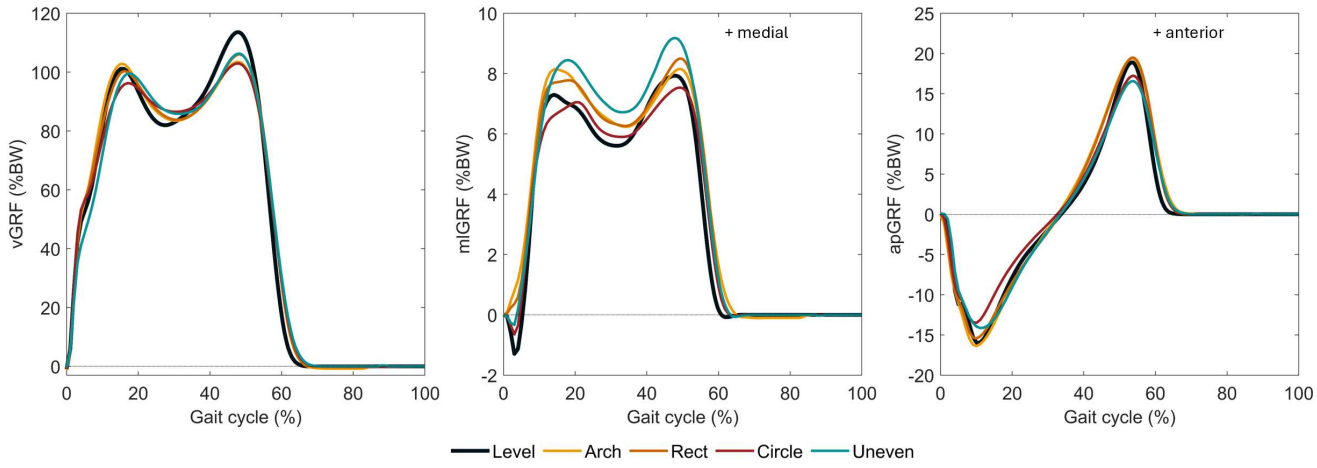


Figure 6. Mean values of the components of the ground reaction force (GRF) vector in the three planes: from left to right, mean values of the vertical component (vGRF) in the sagittal plane, the mediolateral component (mlGRF) in the frontal plane, and the antero–posterior component (apGRF) in the transverse plane.

	Level	Arch	Rectangle	Circle	Uneven	Uneven4line
ROM (deg)						
HX-to-FF	26.4 ± 5.2	21.1 ± 6.0	22.2 ± 4.9	22.7 ± 6.0	18.1 ± 5.2*	18.0 ± 5.8*
FF-to-HF	19.2 ± 4.6	14.8 ± 4.8*	15.2 ± 4.2*	15.1 ± 5.3*	15.4 ± 3.6*	14.4 ± 4.3*
HF-to-TB	17.1 ± 4.1	14.1 ± 2.9*	13.8 ± 3.3*	16.4 ± 3.5	15.5 ± 3.6*	13.6 ± 3.1*
FF-to-TB	33.6 ± 6.7	26.3 ± 6.2*	26.3 ± 5.6*	28.5 ± 6.7*	28.1 ± 5.9*	26.0 ± 5.5*
Ankle	27.6 ± 6.2	23.3 ± 4.8*	22.5 ± 4.7*	24.9 ± 5.9	23.8 ± 4.5*	22.7 ± 5.3
Knee	49.1 ± 9.8	49.1 ± 8.6	50.2 ± 9.5	48.7 ± 9.1	52.0 ± 8.9	48.0 ± 11.3
Hip	38.4 ± 10.3	40.0 ± 9.8	40.9 ± 10.1*	39.6 ± 9.4	41.0 ± 9.3*	36.2 ± 13.5
Angles (deg)						
HX-to-FF DF	11.4 ± 10.3	2.7 ± 11.0*	3.0 ± 9.5*	2.6 ± 10.4*,†	3.0 ± 9.4*,†	1.4 ± 9.3*
FF-to-HF DF	9.7 ± 3.4	6.0 ± 3.3	6.8 ± 2.6	6.8 ± 3.3	5.7 ± 7.6	3.2 ± 8.8
FF-to-HF PF	-9.4 ± 6.0	-6.2 ± 3.4	-6.3 ± 3.0	-7.1 ± 4.0	-9.0 ± 9.0	-9.1 ± 6.4
HF-to-TB lr	-1.8 ± 4.8	0.1 ± 3.9*,†	3.7 ± 3.6*	2.2 ± 4.0*	1.0 ± 7.2	3.5 ± 8.7
HF-to-TB DF	12.6 ± 3.9	19.4 ± 3.9	13.2 ± 4.1	13.9 ± 4.6	15.3 ± 6.2	14.9 ± 5.2
HF-to-TB PF	-2.4 ± 6.6	-4.1 ± 5.5*	1.0 ± 6.1	0.6 ± 6.8	3.2 ± 7.8	3.5 ± 8.9
FF-to-TB lr	-5.0 ± 5.0	0.1 ± 7.3	-1.4 ± 3.8	-1.9 ± 5.6	-6.1 ± 5.9	-3.5 ± 5.8
FF-to-TB DF	21.8 ± 2.6	19.4 ± 5.0	19.6 ± 5.2	20.2 ± 4.4	20.6 ± 4.8	17.4 ± 6.6
FF-to-TB PF	-11.3 ± 6.8	-4.1 ± 5.0*	-4.5 ± 6.0*	-5.9 ± 7.0	-5.7 ± 7.1*	-4.3 ± 5.9*
Ankle lr	1.3 ± 7.3	5.9 ± 3.7	5.1 ± 3.8	3.0 ± 7.1	0.8 ± 5.0	3.3 ± 4.9
Ankle DF	21.5 ± 3.9	22.0 ± 5.3	21.6 ± 5.3	19.6 ± 7.1	21.6 ± 4.1	20.3 ± 5.3
Ankle PF	-5.3 ± 5.3	1.8 ± 5.6*	1.3 ± 6.4*	-2.3 ± 10.5†	-0.2 ± 5.6*	1.5 ± 6.0*
Knee lr	13.8 ± 6.3	19.7 ± 6.2*	19.8 ± 6.1*	18.7 ± 6.3*	17.4 ± 8.3*	17.4 ± 7.6
Knee FX	50.4 ± 11.4	52.6 ± 10.8	53.5 ± 10.6	53.1 ± 11.2	56.1 ± 11.3*	51.8 ± 14.0
Knee EXT	2.0 ± 5.4	6.2 ± 5.1*	4.3 ± 5.6*	6.0 ± 6.5*,†	4.0 ± 5.8*	5.0 ± 6.6*
Hip FX	28.7 ± 8.6	32.0 ± 8.5*	32.3 ± 8.8*	31.7 ± 8.5	32.2 ± 10.2*	27.7 ± 13.4
Hip EXT	-12.5 ± 9.3	-10.6 ± 8.7	-11.5 ± 9.2	-10.0 ± 9.4	-11.3 ± 9.5†	-5.8 ± 12.1
Torques (Nm/kg)						
Ankle lr	-0.2 ± 0.2	-0.1 ± 0.1	-0.1 ± 0.1*	-0.1 ± 0.2	-0.1 ± 0.1*	-
Ankle PF	1.7 ± 0.3	1.3 ± 0.3*	1.3 ± 0.3*	1.3 ± 0.3*	1.5 ± 0.3*	-
Knee lr	0.4 ± 0.3	0.5 ± 0.2	0.5 ± 0.2	0.5 ± 0.3	0.4 ± 0.3	-
Knee EXT	0.2 ± 0.1	0.2 ± 0.2	0.2 ± 0.1	0.2 ± 0.1	0.1 ± 0.0	-
Knee FX	-0.3 ± 0.3	-0.1 ± 0.2*	-0.2 ± 0.3*	-0.2 ± 0.3*	-0.2 ± 0.3*	-
Hip EXT	0.4 ± 0.3	0.3 ± 0.3	0.4 ± 0.3	0.5 ± 0.3	0.4 ± 0.3	-
Hip FX	-0.5 ± 0.3	-0.6 ± 0.3	-0.6 ± 0.3	-0.5 ± 0.3	-0.6 ± 0.3	-
Power (W/kg)						
Ankle dissipation	-0.9 ± 0.3	-0.4 ± 0.3*	-0.5 ± 0.2*	-0.4 ± 0.3*	-0.6 ± 0.2*	-
Ankle generation	3.3 ± 1.1	1.6 ± 0.5*	1.9 ± 0.5*	2.1 ± 0.7*	2.0 ± 0.7*	-
Knee lr	-0.6 ± 0.4	-0.8 ± 0.4	-0.8 ± 0.6	-0.7 ± 0.5	-0.5 ± 0.6	-
Knee generation	0.3 ± 0.2	0.4 ± 0.3	0.4 ± 0.3	0.3 ± 0.2	0.2 ± 0.3	-
Knee stance dissipation	-0.6 ± 0.2	-0.8 ± 0.3	-0.9 ± 0.3	-0.7 ± 0.5	-0.4 ± 0.5	-
Knee dissipation	-0.8 ± 0.4	-0.9 ± 0.5	-1.0 ± 0.4*	-1.1 ± 0.5*	-0.9 ± 0.4	-
Hip dissipation	-0.5 ± 0.2	-0.6 ± 0.2	-0.6 ± 0.2	-0.6 ± 0.2	-0.6 ± 0.2	-
Hip generation	1.0 ± 0.6	0.9 ± 0.4	1.0 ± 0.5	0.9 ± 0.5	0.7 ± 0.4*	-
GRF (%BW)						
apGRF braking peak	-16.0 ± 4.0	-16.4 ± 4.3	-15.4 ± 4.4	-13.5 ± 4.1	-14.2 ± 4.7	-
apGRF propulsive peak	19.0 ± 4.9	19.4 ± 4.0	19.5 ± 4.6	17.3 ± 4.7	16.6 ± 5.6	-
mlGRF 1st peak	7.3 ± 1.6	8.1 ± 1.6*	7.8 ± 1.6	7.1 ± 1.4	8.5 ± 1.9	-
mlGRF 2nd peak	7.9 ± 1.7	8.2 ± 1.7	8.5 ± 1.8	7.5 ± 1.5	9.2 ± 1.9	-
vGRF 1st peak	101.2 ± 15.3	102.8 ± 17.6	100.4 ± 16.7	96.3 ± 15.8*	99.6 ± 16.3*	-
vGRF 2nd peak	113.6 ± 18.5	103.5 ± 16.9*	106.1 ± 17.9*	103.0 ± 17.2*	106.3 ± 18.1*	-

Table 2. From top to bottom: sagittal range of motion (ROM) of all the joints analyzed in the paper (HX-to-FF, hallux-to-forefoot; FF-to-HF, forefoot-to-hindfoot; HF-to-TB, hindfoot-to-tibia; FF-to-TB, forefoot-to-tibia; ankle; knee; hip); values of local maxima and minima of sagittal joint angles, torques, powers, and ground reaction force (GRF). DF, dorsiflexion peak; PF, plantarflexion peak; lr, loading response peak; FX flexion peak; EXT extension peak. GRF, torques, and powers are lacking for the four panels placed in a row as dynamic data are not available for this task. Statistically significant differences from level walking ($p < 0.05$) are indicated with (*). Significant correlations between subject-specific changes in Froude number and changes in kinematic and kinetic parameters (Spearman's rank, $p < 0.05$) are indicated with (†).

Discussion

This study investigated the motion of the complex multi-articular structure of the foot during obstacle negotiation and indoor-simulated uneven terrain walking, and the compensatory strategies adopted by the lower limbs to ensure stability.

We hypothesized increased foot segmental motion to conform to the ground profile, reflecting a need for greater adaptability during stance. Specifically, we expected greater dorsiflexion of proximal foot segments relative to the tibia and greater plantarflexion of distal segments relative to more proximal ones. The results partially supported this hypothesis, showing a segment- and task-dependent response.

Walking on non-flat grounds increased plantarflexion in the hallux-to-forefoot and forefoot-to-hindfoot angles during stance, and markedly reduced dorsiflexion peaks: the forefoot-to-hindfoot dorsiflexion peak decreased by 30-70% during push-off, and the hallux-to-forefoot dorsiflexion peak decreased by over 80% on uneven terrain. In contrast, hindfoot-to-tibia dorsiflexion increased during the first half of the stance on obstacles, especially the arched one, consistent with a rapid adjustment of the hindfoot at initial contact to the shape and incline of the obstacle. This trend towards dorsiflexion during loading response was less evident on continuous uneven ground, which is lower than the discrete obstacles and over which the load is likely distributed more gradually. A more pronounced dorsiflexion increase was observed during the first half of stance in the forefoot-to-tibia angle, with effects depending on disturbance shape and height. Interestingly, the influence of obstacle shape in the first half of stance was clearly visible in hindfoot- and forefoot-to-tibia angles, whereas it was more limited in forefoot-to-hindfoot angle, suggesting reduced midfoot sensitivity to the ground profile during this phase.

Across all non-flat conditions, foot segment ROM decreased compared with level walking (Table 2), rather than increasing to conform to the ground profile. Reduced hindfoot-to-tibia and forefoot-to-tibia motion may reflect constraints imposed by obstacle inclination and shape, which alter the ankle kinematics required to advance the centre of mass over the foot. Overall, this reduction in ROM suggests a stiffening strategy of the foot segments in response to irregular grounds, potentially functioning as a clutch-like mechanism to increase grip and stability during stance by maximizing surface contact on non-painful obstacles. The greater ROM reduction on lined-up uneven panels - where the panels are lower than discrete obstacles and lack a well-defined shape to which the foot can conform - compared with single obstacles suggests that repeated perturbations may promote a more conservative stabilization strategy. In this condition, the increased plantarflexion of the forefoot relative to the hindfoot may reflect stiffening along the longitudinal arch, representing a compensatory mechanism to maintain robustness when precise foot conformability is limited. This behaviour may also be partially influenced by the discomfort experienced by participants when walking barefoot on those panels.

In the frontal and transverse planes, hindfoot and forefoot angles relative to the tibia showed increased eversion/pronation and external rotation/abduction on obstacles, possibly related to altered subtalar joint mechanics and limited plantar arch extension due to obstacles.

We initially hypothesized that challenging terrains would reduce ankle joint ROM and increase knee flexion to facilitate foot-ground interaction. The results generally support this hypothesis, although the observed adaptations were terrain dependent.

Ankle ROM decreased across all non-flat conditions: plantarflexion during loading response was markedly reduced - nearly absent for larger obstacles, whereas dorsiflexion increased over most of stance, consistent with hindfoot/forefoot angles relative to the tibia. Despite this, dorsiflexion peak values remained close to level walking, while plantarflexion peaks were significantly reduced and often remained within dorsiflexion. This behaviour likely reflects the mechanical constraint imposed by obstacle inclination, as achieving level-walking plantarflexion would increase forward displacement of the centre of mass and potentially destabilize the body during propulsion. The small increase in stance eversion and external rotation in the frontal and transverse planes, respectively, suggests multi-planar adaptations for stability on irregular surfaces.

Knee ROM remained relatively consistent across conditions, with only a slight increase on the rectangular obstacle and uneven terrain. However, stance knee flexion increased significantly on non-flat grounds, enhancing compliance to accommodate obstacles and helping keep the COM aligned over the base of support to mitigate the risk of instability. Similarly, the significant increase in stance hip flexion represents an additional compensatory strategy for safe obstacle negotiation. Increased knee and hip flexion during swing, combined with ankle dorsiflexion, likely enhanced toe-ground clearance.

We hypothesized that stepping onto obstacles would require greater ankle joint torque and increased negative power at the knee, reflecting the need for energy absorption during increased knee flexion. The results support these hypotheses, showing significant adaptations in lower limb joint kinetics when walking on non-flat grounds.

Dynamically, challenging terrains increased ankle plantarflexor moment during the first half of stance. This moment scaled with obstacle size, with larger obstacles demanding greater plantarflexor activity, consistent with the increased effort to accommodate irregularities. During the second half of stance, the plantarflexor moment was significantly reduced, leading to a lower moment peak, especially for larger obstacles. This may relate to obstacle height and inclination reducing the GRF lever arm during terminal stance and push-off, and promoting forward COM displacement, reducing the need for active push-off. In addition, the reduced plantarflexor peak was associated with a diminished second vGRF peak, indicating lower limb loading on non-flat ground. Consequently, also ankle push-off power generation decreased significantly (about 50% decrease compared

with level walking), suggesting reduced propulsion under unstable or sloped conditions.

At the knee, the tendency towards an extensor moment pattern during stance on obstacles, consistent with the increased knee flexion, and the increased energy absorption peaks reflect the damping role of the knee, dissipating additional mechanical energy introduced by terrain irregularity and height. Hip kinetics showed modest increases in extensor moment, associated with greater flexion, and energy absorption on obstacles, particularly at the beginning and end of stance. Overall, these joint-level kinetic adaptations indicate a redistribution of mechanical work, with increased energy dissipation - especially at the knee - at the expense of ankle propulsion. This is consistent with our initial hypothesis and highlights how the body adjusts joint function to maintain control and stability on non-flat ground.

The reduced second vGRF peak (up to 10% for the circular obstacle) suggests increased difficulty in loading the limb on irregular terrains during the second half of stance, typically leading to greater contralateral limb loading. Reduced braking/propulsive apGRF peaks on the circular obstacle and uneven terrain suggest a more vertically aligned limb during stance. This interpretation may be consistent with participants' feedback, as these tasks were reported to be the most difficult and painful to perform barefoot, possibly inducing compensatory strategies such as shorter steps and a more upright limb alignment.

Participants were asked to walk at their self-selected speed to avoid distortions in kinematics or kinetics associated with enforced speed. Speed analysis indicated that the observed differences between level and obstacle walking were not primarily driven by changes in normalized walking speed. Moreover, foot segment kinematics for level walking was consistent with previous studies employing the Oxford Foot Model or other multi-segment foot models[11,17,39]. This further supports the interpretation that the observed differences are mainly attributable to terrain characteristics rather than variations in walking speed.

Some study limitations should be considered when interpreting the results. These include the restricted set of obstacles and indoor terrains relative to the full variability of daily-life environments. Future work should include a wider range of terrains and walking conditions, potentially leveraging dedicated test beds recently developed for assessing lower-limb wearable devices on uneven-terrains[40], and extend to out-of-the-laboratory experiments to enable assessment in continuous and uncontrolled environments. Trunk kinematics was not recorded and could provide insight into regulation of body's angular momentum for balance. Finally, unconstrained foot placement on obstacles introduced variability in foot contact regions and orientation across participants and tasks. Hence, methods to classify foot placement on obstacles could improve inter-subject comparisons of foot deformation and reduce bias related to individual walking strategies. This is consistent with challenges reported in a previous study on prosthetic users walking on uneven terrain, which highlighted the difficulty of accounting for foot orientation and the need for methods to assess step similarity on irregular surfaces[41].

Conclusions

This work investigated how the human foot modifies its shape to adapt to irregular ground profiles and the compensatory strategies adopted by the lower limbs.

Greater plantarflexion of the hallux and forefoot, and their reduced dorsiflexion peaks, greater dorsiflexion of forefoot and hindfoot relative to the tibia, and an overall reduction in foot segment ROM were observed, suggesting a stiffening mechanism that enhances grip and stability rather than flexibility. Ankle motion was reduced, while knee and hip flexion increased over stance to improve compliance and maintain the centre of mass over the base of support. Ankle plantarflexor torque increased during the first half of stance to overcome obstacles, whereas push-off plantarflexion torque peak and power generation were reduced. Increased negative knee power confirmed its damping role, dissipating additional energy introduced by irregular terrain. These compensatory mechanisms indicate that locomotion on non-level ground involves a redistribution of work across joints to ensure safe and stable locomotion: the foot stiffens to stabilize surface contact, the ankle overcomes the unevenness and controls the COM motion, while the knee and hip increase flexion and energy absorption. Overall, the body transitions from a propulsion-oriented strategy on level ground to a stabilization and energy dissipation-oriented strategy on uneven surfaces, ensuring safe and stable locomotion.

The dataset generated in this study provides valuable insights into foot mobility across various terrains and may inform the design of adaptive artificial feet to improve stability for robots and prosthetic users on unstructured terrains.

Data availability

The dataset generated and analysed during the current study is available from the corresponding author on reasonable request.

References

1. Holowka, N. B. & Lieberman, D. E. Rethinking the evolution of the human foot: Insights from experimental research. *J. Exp. Biol.* **221**, 174425, DOI: 10.1242/jeb.174425 (2018).

2. Holowka, N. B., O'Neill, M. C., Thompson, N. E. & Demes, B. Chimpanzee and human midfoot motion during bipedal walking and the evolution of the longitudinal arch of the foot. *J. Hum. Evol.* **104**, 23–31, DOI: https://doi.org/10.1016/j.jhevol.2016.12.002 (2017).

3. Venkadesan, M., Bandi, M. M. & Mandre, S. *Biological feet: Evolution, mechanics and applications* (Elsevier Science, 2017).

4. Zelik, K. E. & Honert, E. C. Ankle and foot power in gait analysis: Implications for science, technology and clinical assessment. *J. Biomech.* **75**, 1–12, DOI: 10.1016/J.JBIOMECH.2018.04.017, (2018).

5. Voloshina, A. S., Kuo, A. D., Daley, M. A. & Ferris, D. P. Biomechanics and energetics of walking on uneven terrain. *J. Exp. Biol.* **216**, 3963 – 3970, DOI: 10.1242/jeb.081711 (2013).

6. Voloshina, A. S. & Ferris, D. P. Biomechanics and energetics of running on uneven terrain. *J. Exp. Biol.* **218**, 711 – 719, DOI: 10.1242/jeb.106518 (2015).

7. Kowalsky, D. B., Rebula, J. R., Ojeda, L. V., Adamczyk, P. G. & Kuo, A. D. Human walking in the real world: Interactions between terrain type, gait parameters, and energy expenditure. *PLoS ONE* **16**, e0228682, DOI: 10.1371/journal.pone.0228682 (2021).

8. Gates, D. H., Wilken, J. M., Scott, S. J., Sinitski, E. H. & Dingwell, J. B. Kinematic strategies for walking across a destabilizing rock surface. *Gait Posture* **35**, 36 – 42, DOI: 10.1016/j.gaitpost.2011.08.001 (2012).

9. Leardini, A., Caravaggi, P., Theologis, T. & Stebbins, J. Multi-segment foot models and their use in clinical populations. *Gait & Posture* **69**, 50–59, DOI: 10.1016/J.GAITPOST.2019.01.022 (2019).

10. Pohl, M. B., Messenger, N. & Buckley, J. G. Forefoot, rearfoot and shank coupling: Effect of variations in speed and mode of gait. *Gait Posture* **25**, 295–302, DOI: 10.1016/J.GAITPOST.2006.04.012 (2007).

11. Hunt, A. E., Smith, R. M., Torode, M. & Keenan, A. M. Inter-segment foot motion and ground reaction forces over the stance phase of walking. *Clin. Biomech.* **16**, 592–600, DOI: 10.1016/S0268-0033(01)00040-7 (2001).

12. Leardini, A. *et al.* Rear-foot, mid-foot and fore-foot motion during the stance phase of gait. *Gait Posture* **25**, 453–462, DOI: 10.1016/J.GAITPOST.2006.05.017 (2007).

13. Simon, J. *et al.* The heidelberg foot measurement method: Development, description and assessment. *Gait & Posture* **23**, 411–424, DOI: 10.1016/J.GAITPOST.2005.07.003 (2006).

14. Dubbeldam, R., Nester, C., Nene, A. V., Hermens, H. J. & Buurke, J. H. Kinematic coupling relationships exist between non-adjacent segments of the foot and ankle of healthy subjects. *Gait Posture* **37**, 159–164, DOI: 10.1016/J.GAITPOST.2012.06.033 (2013).

15. Takabayashi, T. *et al.* Changes in kinematic coupling among the rearfoot, midfoot, and forefoot segments during running and walking. *J. Am. Podiatric Med. Assoc.* **108**, 45–51, DOI: 10.7547/16-024 (2018).

16. Chang, R., Emmerik, R. V. & Hamill, J. Quantifying rearfoot-forefoot coordination in human walking. *J. Biomech.* **41**, 3101–3105, DOI: 10.1016/J.JBIOMECH.2008.07.024 (2008).

17. Sun, D., Fekete, G., Mei, Q. & Gu, Y. The effect of walking speed on the foot inter-segment kinematics, ground reaction forces and lower limb joint moments. *PeerJ* **2018**, e5517, DOI: 10.7717/PEERJ.5517/SUPP-3 (2018).

18. Dixon, P. C., Böhm, H. & Döderlein, L. Ankle and midfoot kinetics during normal gait: A multi-segment approach. *J. Biomech.* **45**, 1011–1016, DOI: 10.1016/J.JBIOMECH.2012.01.001 (2012).

19. Morio, C., Lake, M. J., Gueguen, N., Rao, G. & Baly, L. The influence of footwear on foot motion during walking and running. *J. Biomech.* **42**, 2081–2088, DOI: 10.1016/J.JBIOMECH.2009.06.015 (2009).

20. Azevedo, A. M., Oliveira, R., Vaz, J. R. & Cortes, N. Oxford foot model kinematics in landings: A comparison between professional dancers and non-dancers. *J. Sci. Medicine Sport* **23**, 347 – 352, DOI: 10.1016/j.jsams.2019.10.018 (2020).

21. Pothrat, C., Authier, G., Viehweger, E., Berton, E. & Rao, G. One- and multi-segment foot models lead to opposite results on ankle joint kinematics during gait: Implications for clinical assessment. *Clin. Biomech.* **30**, 493 – 499, DOI: 10.1016/j.clinbiomech.2015.03.004 (2015).

22. Carson, M. C., Harrington, M. E., Thompson, N., O'Connor, J. J. & Theologis, T. N. Kinematic analysis of a multi-segment foot model for research and clinical applications: a repeatability analysis. *J Biomech* **34**, 1299–307, DOI: 10.1016/s0021-9290(01)00101-4 (2001).

23. Novak, A. C., Mayich, D. J., Perry, S. D., Daniels, T. R. & Brodsky, J. W. Gait analysis for foot and ankle surgeons—topical review, part 2: Approaches to multisegment modeling of the foot. *Foot & Ankle Int.* **35**, 178–191, DOI: 10.1177/1071100713511435 (2014). PMID: 24334310, https://doi.org/10.1177/1071100713511435.

24. Baker, R., Leboeuf, F., Reay, J. & Sangeux, M. *The Conventional Gait Model - Success and Limitations*, 1–19 (Springer International Publishing, Cham, 2017).

25. Carty, C. P., Walsh, H. P. & Gillett, J. G. Sensitivity of the oxford foot model to marker misplacement: A systematic single-case investigation. *Gait & Posture* **42**, 398–401, DOI: 10.1016/J.GAITPOST.2015.06.189 (2015).

26. Curtis, D. J., Bencke, J., Stebbins, J. A. & Stansfield, B. Intra-rater repeatability of the oxford foot model in healthy children in different stages of the foot roll over process during gait. *Gait & Posture* **30**, 118–121, DOI: 10.1016/J.GAITPOST.2009.02.013 (2009).

27. Lucareli, P. R. G. *et al.* Repeatability of a 3d multi-segment foot model during anterior and lateral step down tests. *Gait & Posture* **43**, 9–16, DOI: 10.1016/J.GAITPOST.2015.10.008 (2016).

28. McCahill, J., Stebbins, J., Koning, B., Harlaar, J. & Theologis, T. Repeatability of the oxford foot model in children with foot deformity. *Gait & Posture* **61**, 86–89, DOI: 10.1016/J.GAITPOST.2017.12.023 (2018).

29. van Hoeve S *et al.* Repeatability of the oxford foot model for kinematic gait analysis of the foot and ankle. *Clin. Res. on Foot & Ankle 2015 3:2* **3**, 1–8, DOI: 10.4172/2329-910X.1000171 (2015).

30. Wright, C. J., Arnold, B. L., Coffey, T. G. & Pidcoe, P. E. Repeatability of the modified oxford foot model during gait in healthy adults. *Gait & Posture* **33**, 108–112, DOI: 10.1016/J.GAITPOST.2010.10.084 (2011).

31. Milner, C. E. & Brindle, R. A. Reliability and minimal detectable difference in multisegment foot kinematics during shod walking and running. *Gait & Posture* **43**, 192–197, DOI: 10.1016/J.GAITPOST.2015.09.022 (2016).

32. Shono, H. *et al.* Determination of relationship between foot arch, hindfoot, and hallux motion using oxford foot model: Comparison between walking and running. *Gait Posture* **92**, 96 – 102, DOI: 10.1016/j.gaitpost.2021.10.043 (2022).

33. Plug-in gait reference guide (2016-2023).

34. Pace, A. *et al.* An experimental setup to test obstacle-dealing capabilities of prosthetic feet. In *2023 International Conference on Rehabilitation Robotics (ICORR)*, 1–6, DOI: 10.1109/ICORR58425.2023.10304763 (2023).

35. Lordall, J., Oates, A. R. & Lanovaz, J. L. Spatiotemporal walking performance in different settings: effects of walking speed and sex. *Front. Sports Active Living* **6**, 1277587, DOI: 10.3389/FSPOR.2024.1277587/BIBTEX (2024).

36. Kao, P. C. & Pierro, M. A. Dual-task treadmill walking at self-paced versus fixed speeds. *Gait & Posture* **89**, 92–101, DOI: 10.1016/J.GAITPOST.2021.07.001 (2021).

37. Orekhov, G., Robinson, A. M., Hazelwood, S. J. & Klisch, S. M. Knee joint biomechanics in transtibial amputees in gait, cycling, and elliptical training. *PLOS ONE* **14**, e0226060, DOI: 10.1371/journal.pone.0226060 (2019).

38. Perry, J. & Burnfield, J. *Gait Analysis: Normal and Pathological Function* (SLACK Incorporated, New Jersey, 2010), 2nd edn.

39. Tulchin, K., Orendurff, M., Adolfsen, S. & Karol, L. The effects of walking speed on multisegment foot kinematics in adults. *J. Appl. Biomech.* **25**, 377–386, DOI: 10.1123/JAB.25.4.377 (2009).

40. Cwa 17664:2021 lower-limb wearable devices – performance test method for walking on uneven terrain. Tech. Rep., CEN Workshop Agreement (2021).

41. McDonald, K. A., Teater, R. H., Cruz, J. P. & Zelik, K. E. Unilateral below-knee prosthesis users walking on uneven terrain: The effect of adding a toe joint to a passive prosthesis. *J. Biomech.* **138**, 111115, DOI: https://doi.org/10.1016/j.jbiomech.2022.111115 (2022).

Funding

This research received funding from the RAISE Project "Robotics and AI for Socio-economic Empowerment" (ECS_00000035 CUP J33C22001220001).

Author contributions

A.P., M.C., G.Gr., and M.G.C. conceived the experiment, A.P., M.C., and G.Ge., conducted the experiment, A.P., M.C., and G.Ge. analysed the results. E.P., A.B., and M.G.C. supervised the work. All authors reviewed and edited the manuscript and gave final approval for publication.

Competing interests

The authors declare no competing interests.

Additional information

A Supplementary Information file is available.

Supplementary Files

This is a list of supplementary files associated with this preprint. Click to download.

- FootSegmentsMotionduringUnevenTerrainWalkingInfluenceonLowerLimbBiomechanicssupplmat.pdf